

UC Berkeley

UC Berkeley Previously Published Works

Title

Estimation of soil classes and their relationship to grapevine vigor in a Bordeaux vineyard: advancing the practical joint use of electromagnetic induction (EMI) and NDVI datasets for precision viticulture

Permalink

<https://escholarship.org/uc/item/2t70w418>

Journal

Precision Agriculture, 22(4)

ISSN

1385-2256

Authors

Hubbard, Susan S
Schmutz, Myriam
Balde, Abdoulaye
[et al.](#)

Publication Date

2021-08-01

DOI

10.1007/s11119-021-09788-w

Peer reviewed



Estimation of soil classes and their relationship to grapevine vigor in a Bordeaux vineyard: advancing the practical joint use of electromagnetic induction (EMI) and NDVI datasets for precision viticulture

Susan S. Hubbard¹ · Myriam Schmutz² · Abdoulaye Balde^{2,3} · Nicola Falco¹ · Luca Peruzzo¹ · Baptiste Dafflon¹ · Emmanuel Léger⁴ · Yuxin Wu¹

Accepted: 7 January 2021

© This is a U.S. government work and not under copyright protection in the U.S.; foreign copyright protection may apply 2021

Abstract

Working within a vineyard in the Pessac Léognan Appellation of Bordeaux, France, this study documents the potential of using simple statistical methods with spatially-resolved and increasingly available electromagnetic induction (EMI) geophysical and normalized difference vegetation index (NDVI) datasets to accurately estimate Bordeaux vineyard soil classes and to quantitatively explore the relationship between vineyard soil types and grapevine vigor. First, co-located electrical tomographic tomography (ERT) and EMI datasets were compared to gain confidence about how the EMI method averaged soil properties over the grapevine rooting depth. Then, EMI data were used with core soil texture and soil-pit based interpretations of Bordeaux soil types (Brunisol, Redoxisol, Colluviosol and Calcosol) to estimate the spatial distribution of geophysically-identified Bordeaux soil classes. A strong relationship ($r=0.75$, $p<0.01$) was revealed between the geophysically-identified Bordeaux soil classes and NDVI (both 2 m resolution), showing that the highest grapevine vigor was associated with the Bordeaux soil classes having the largest clay fraction. The results suggest that within-block variability of grapevine vigor was largely controlled by variability in soil classes, and that carefully collected EMI and NDVI datasets can be exceedingly helpful for providing quantitative estimates of vineyard soil and vigor variability, as well as their covariation. The method is expected to be transferable to other viticultural regions, providing an approach to use easy-to-acquire, high resolution datasets to guide viticultural practices, including routine management and replanting.

Keywords Geophysics · Precision viticulture · Electrical conductivity · Electromagnetic Induction (EMI) · NDVI · Hyperspectral · Bordeaux · Vineyard soil · Grapevine vigor

✉ Susan S. Hubbard
sshubbard@lbl.gov

¹ Lawrence Berkeley National Laboratory, Berkeley, CA, USA

² Bordeaux INP - UBM, EA4592 Talence, France

³ SNCF Réseau, Bordeaux, France

⁴ Université Paris-Saclay, CNRS, GEOPS, 91405 Orsay, France

Introduction

Climate change, extreme weather, wildfire, land-use change, and other disturbances are significantly reshaping interactions between the biosphere, geosphere, and hydrosphere, including soil–plant interactions that influence water and biogeochemical cycles. To gain an understanding of soil–plant interactions in both natural and managed ecosystems, and how those interactions may change over time, measurement methods are needed that can provide information about both above and below ground characteristics—with sufficient accuracy, with spatial resolutions relevant to the characteristic lengths scales of soil and plant properties, and over landscape scales. This study explores the value of high resolution surface geophysical and airborne remote sensing data to provide proxy information about soil texture and grapevine vigor (or vegetation biomass), respectively, and to explore the covariability between these soil and plant properties during the growing season.

Given the socioeconomic and cultural importance of vineyards, this study explores the value of increasingly available methods for characterizing soil and plant heterogeneity at a vineyard site in the Bordeaux region of France. Following the French concept of *terroir* (Wilson 1998; van Leeuwen et al. 2004; van Leeuwen and Seguin 2007), winegrapes are an integrator of many influences, including microclimate and soil properties (Bramley et al. 2011; Baciocco et al. 2014; Almaraz 2015). While temperature dynamics are the major driver of grapevine phenology (Parker et al. 2011), smaller-scale spatial variability of soil physical and chemical properties also influences vine performance (e.g., Lanyon et al. 2004). This study is motivated by the need to develop tractable approaches for adequately characterizing vineyard soil properties and their influence on grapevine vigor—in response to increasingly frequent environmental stressors, in high resolution and over scales relevant for guiding management practices.

Diverse approaches exist for characterizing grapevine and grape variability, which provide important information for vineyard management (Bonilla et al. 2015). Typical methods are based on plant-based sampling and analysis, including quantifying the number of grape-bearing vines per acre, the number of grape clusters per vine, and cluster weight (Wolpert and Vilas 1992). Both direct and indirect approaches have been used to estimate grapevine vigor. Common direct approaches include measuring Leaf Area Index (LAI), which involves cutting leaves (Anderson et al. 2004), as well as assessing pruning weights. Remote sensing methods are used increasingly to estimate the spatial distribution of grapevine vigor (Das et al. 2015), including spectral radiance approaches that measure in the near-infrared portion of the electromagnetic frequency spectrum.

Compared to conventional sampling-based techniques, remotely sensed data acquired in vineyards are typically advantageous for estimating grapevine vigor because they can provide estimates over large areas in a non-invasive manner. Johnson et al. (2003) used high-spatial resolution Normalized Difference Vegetation Index (NDVI) imagery to estimate grapevine LAI over large regions. They showed that remotely-sensed vineyard LAI can provide input into plant growth models that can be used to guide canopy management. Time-lapse satellite-based vegetation indices can also be used to track grapevine development (Cunha et al. 2010; Hall et al. 2002). Sun et al. (2017) used periodic LAI measurements and NDVI to estimate grape yield in California vineyards. They found that NDVI and LAI had similar performance as a predictor of spatial yield variability, providing peak correlations during the growing season. They also identified factors (such as slope, management practices, and weather) that influenced the NDVI data and thus the prediction of yield spatial variability.

Soil properties are recognized as important for grapevine development and grape phenolic development (Lanyon et al. 2004; Van Leeuwen et al. 2004; White 2015). Soil texture influences the amount of water a soil can hold and the rate that water and dissolved nutrients can be taken up by the plant (Proffitt and Campbell-Clause 2012). As soils vary laterally due to natural geologic processes, grapevine variability can similarly vary laterally over short distances. Vineyard soils encompass a wide range of textures (Baize and Girard 1998, 2008). Vineyard soil classification maps, also referred to as pedological maps, are traditionally performed by digging soil pits, followed by a qualitative description of soil horizons of a given area (Van Leeuwen and Chery 2001). Spatial interpolation of pit measurements is commonly performed to create a vineyard pedological map. Soil pit characterization is destructive, time-consuming and expensive. For this reason, vineyard soil pits are typically sparse (Van Leeuwen and Chery 2001), leading to distances between soil property information that are often much greater than the characteristic length scales of natural soil texture spatial variability (Hubbard et al. 2006).

Lateral variations in soil properties are a function of topographical, geological, climate and land management processes and thus will vary with region. Small-scale lateral variability can pose a challenge for viticulturalists, who strive for uniformity of winegrape characteristics within vineyard blocks, which are vineyard management parcels. Geophysical methods hold promise for providing information about within-block soil property variability in a minimally invasive manner, as has been described by previous studies (Hubbard et al. 2006; Bramley and Hamilton 2007; Imre et al. 2013). Grote et al. (2003) and Hubbard et al. (2002) demonstrated the value of Ground Penetrating Radar (GPR) groundwave measurements for estimating the spatial variability of vineyard soil water content variability. Grote et al. (2010) showed how time-lapse GPR soil moisture information can be used to estimate shallow vineyard soil texture. Grote et al. (2003, 2010) estimated characteristic lengths of lateral soil property variability in Napa Valley, revealing substantial lateral variations in soil properties over decimeters to decameters. Lunt et al. (2005) demonstrated the value of GPR reflected wave information for quantifying vineyard soil moisture, and documented a correspondence between deep vineyard soil moisture content and vineyard vegetation density. While GPR can provide significant information about vineyard soil variability, the data processing required to extract relevant information can be challenging for practitioners.

A number of studies have also explored the value of electrical geophysical methods, including electromagnetic induction method (EMI) and electrical resistivity tomography (ERT), for providing spatially extensive information about vineyard soil properties. The apparent electrical conductivity (ECa) of geologic materials is influenced by many factors, including soil water content, compaction, porosity, temperature, clay content, and salinity. In particular, soil water content and soil texture (Brevik and Fenton 2015; Stednick et al. 2006) significantly influence the effective soil ECa. Due to its ease of use, EMI has been most widely deployed to explore the relationship between ECa and soil texture in agricultural studies. EMI approaches yield spatially resolved yet depth-averaged estimates of soil electrical conductivity. A single depth integrated ECa value provided at a specific location from EMI is based on a number of factors, including soil properties and depth sensitivity of the geophysical measurement. The majority of vineyard studies that demonstrated a good correlation between vineyard soil ECa and soil texture were performed using the EM38 system and soil samples, both sampling the upper ~30 cm of the soil column (e.g., Hedley et al. 2004; Rodriguez Perez et al. 2011; Bonfante et al. 2015). However, other studies have found poor relationships, and have attributed them to aspects such as soil compaction (André et al. 2012), interference from metal trellis wires (e.g., Lamb et al. 2005; Coulouma

et al. 2010), and underground infrastructure (André et al. 2012). A universal relationship between EMI-derived ECa and soil texture does not exist for viticulture, and climate and yield have been identified as important for considering transferability of a developed soil EC-texture relationships (Heil and Schmidhalter 2017). Geophysical-derived estimates of soil ECa have also been used to address other viticultural objectives besides estimation of soil property variability. For example, Goulet and Barbeau (2006) used soil electrical resistivity to analyze the influence of vineyard grass cover on the spatial distribution of soil moisture and rootstock and Bonfante et al. (2015) used electrical methods to delineate vineyard microzones.

Only a few studies have investigated the relationship between soil and grapevine variability using surface EMI and airborne NDVI. These studies have met with mixed results. Working in a vineyard in the south of France, André et al. (2012) performed high-resolution imaging of vineyard soils (using GPR, EMI and apparent resistivity profiling). They collected EMI data using an ARP system (which provided averaged ECa estimates over depth ranges of ~0.8 to ~2.2 m) as well as high resolution (0.1 m) NDVI data. The EMI data revealed significant heterogeneity in soil ECa. While they did not collect soil samples, they found that the spatial patterns of soil ECa were similar to patterns of vineyard soil classifications revealed from maps, as well as with stratigraphic information obtained from GPR data. They provided a cross-plot between co-located NDVI and EMI ECa estimates across many vineyard blocks, which did not reveal a relationship between soil and plant proxy measurements at the vineyard scale. However, their study revealed that patterns of NDVI, vineyard soil class and ECa from EMI were similar for specific vineyard blocks. While the André et al. (2012) study indicated the potential for these easy-to-use datasets for delineating vineyard management zones, it also highlighted that compaction and metal infrastructure can influence the EMI-based ECa, and thus inhibit the utility of EMI to consistently characterize vineyard soil variability. Working in two blocks with contrasting soil types located within a well-established and non-irrigated vineyard in Southern France during a dry season, Coulouma et al. (2010) quantitatively explored if EMI information could be used to predict vegetation variability, which would be helpful for quantifying grapevine vigor variability when NDVI data are not available. To characterize the soil, they obtained processed soil ECa maps from Soil Information Systems (SIS), acquired using an EMI sensor towed behind an all-terrain vehicle. While the description of the EMI system was not provided, the depth of investigation of the EMI sensor was reported to be 1 m. The data were collected along transects spaced a few meters apart and subsequently interpolated to 1 m² lateral resolution. They interpreted three different soil classes for each block using the soil cores and expert knowledge of the local environment. NDVI data were collected over the vineyard blocks using an airborne platform with lateral resolution of 1 m². They found a good correlation between ECa and soil classes in one block. However, the other block included a soil unit that likely limited rooting depth but that had similar ECa to surrounding soils. As a result, the relationship between soil classes and EMI-based ECa was poor in that block. Accordingly, EMI ECa maps compared well with NDVI maps in some regions but poor in others. Coulouma et al. (2010) explicitly recommended that future studies should be performed under moist soil conditions in order to enhance EMI-based discrimination of soil variability that could in turn influence grapevine variability.

These studies also suggest the importance of considering the depth zone of imaging when designing geophysical surveys to characterize vineyard soils surrounding grapevine roots. Roots absorb and conduct most of the vine's water and nutrient requirements to the aerial parts of the plant. Grapevine roots can extend deeper than many other agricultural crops. Through analyzing numerous reports of vineyard trench wall profiles,

Smart et al. (2006) reported that ~80% of grapevine roots were in the upper 1 m of the soil column, suggesting that EMI acquisition modes should be use that allow interrogation of at least the first meter below ground surface.

In addition to vineyard-based studies, soil ECa and NDVI have also been used together to evaluate soil–plant interactions in other agricultural as well as in natural ecosystems. Exploring soil and plant interaction in an agricultural site in Germany, von Hebel et al. (2018) quantitatively combined time-lapse, ground-based high resolution (1 m) EMI and airborne hyperspectral data to explore the control of soil on estimated plant photosynthetic rates. A multi-coil EMI system allowed interrogation of soil ECa over several depths of investigation. They found a significant correlation of the inverted depth-specific soil ECa and plant property estimates, and in particular that a ~1 m deep buried paleo river channel greatly influenced plant behavior. Working in the same region, Rudolph et al. (2015) compared LAI estimated from airborne data with soil ECa estimated at different depths using the CMD-MiniExplorer EMI system. They found variable correlations between ECa and LAI ($R^2=0.2$ to 0.82) depending on vineyard block. Their results indicate that the buried paleo-river was predominantly responsible for better crop development in drought periods, likely due to its soil moisture relative to surrounding sediments. Using ERT, point soil sensors, and phenocams, Dafflon et al. (2017) documented a relationship between soil EC, thaw layer thickness, soil moisture, and vegetation vigor during the growing season in a natural Tundra ecosystem In this Arctic system, they found that the spatial distribution of plant greenness at the peak of the growing season could be used to predict the spatial variability of soil properties. Falco et al. (2019) investigated the covariability between plant community distribution and soil properties, showing the existence of a strong correlation between soil ECa spatial variability and plant spatial distribution estimated by high-resolution satellite images.

While climate and weather influence grapevine development and vintage quality at the vineyard to viticultural region scales (e.g., Bios et al. 2018), this study focuses on investigating the influence of soil variability on grapevine vigor over the smaller scales of vineyard management, such as within and across vineyard blocks. This study explores the hypothesis that during the growing season, grapevine vegetation variability within and across vineyard blocks is greatly influenced by soil property variability, and that easy-to-use and increasingly available EMI and NDVI datasets can be used to provide quantitative estimates of vineyard soil texture and grapevine vigor, respectively, and their coverability. To test this hypothesis, the study describes the development and testing of statistical approaches to quantify the relationship between vineyard soil and grapevine vegetation within a Bordeaux region vineyard during the growing season. The objectives of the development and testing of this methodology were to: (1) gain confidence in the use of EMI for quantitative estimation of spatial distribution of Bordeaux soil types; and (2) quantify the relationship between estimated vineyard soil types and grapevine vegetation vigor during the growing season.

This study was designed through explicit consideration of several findings and recommendations from previous studies. Examples include consideration of the proximity of vineyard infrastructure that could detrimentally contribute to the ECa response, the lateral resolution of EMI and NDVI datasets used to estimate soil and plant variability, respectively, and the depth zone of investigation by the EMI method. The period of the study was also a critical part of the design. The study was conducted during an important phenological stage when berries were forming and grapevine vegetation was well developed. The major EMI data acquisition campaigns were also performed during a period where

soil moisture was assumed to be favorable for enhancing discrimination of ECa-based soil variability.

Description of site and key characteristics

The study was carried out in a portion of a vineyard of Château La Louvière, located on the Left Bank of the Gironde River in the Pessac-Léognan Appellation near Bordeaux, France (Fig. 1a). The Bordeaux region is known for cultivation of grapes, including red (Cabernet Franc, Cabernet Sauvignon, Merlot, Petit Verdot and Malbec) and white (Sauvignon Blanc, Semillon and Muscadelle) varieties. The region is close to large bodies of water (the Atlantic Ocean, the Gironde Estuary, and the Garonne and Dordogne Rivers) as well as a forested region, which play an important thermo-regulating role (Baciocco et al. 2014). An oceanic climate prevails, with a mean annual temperature of 12.7 °C and a mean annual rainfall of 800 mm. Precipitation is typically lowest in July, with a monthly average of 52 mm. The highest monthly precipitation occurs in December, with an average of 104 mm. April through September typically marks the Bordeaux winegrape growing season, from budbreak to harvest respectively (Bois et al. 2018). Irrigation is severely

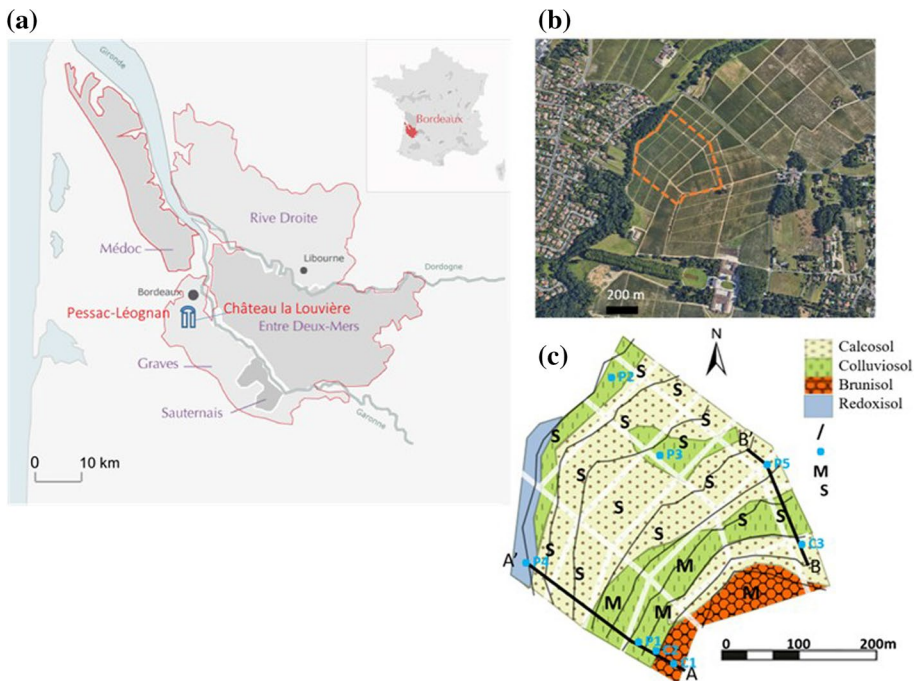


Fig. 1 a Vineyard Study Site at the Château La Louvière in the Pessac-Léognan region of Bordeaux. b Google Earth image showing the study site (dashed orange polygon); c pedological soil map from Château La Louvière, digitized based on a former survey (Tregoat 2007). The two black lines are the positions of the ERT transects: AA' corresponds to the Merlot transect and BB' to the Sauvignon Blanc transect. The white lines delineate the roads that separate vineyard blocks at the study site. Individual grapevine blocks, planted to Merlot (M) and Sauvignon Blanc (S) are indicated. The locations of the Pits (P) and Cores (C) are shown by blue dots (Color figure online)

restricted in Bordeaux and no irrigation was performed during this study. A meteorological station is located very near the study parcel at Château La Louvière, which provided site-specific meteorological information. Air temperature, humidity and precipitation measurements associated with this study are provided in the Supplementary Information.

The heterogeneity of the soil's composition and depth in the Pessac-Léognan region provides a remarkable diversity of expression in the resulting grapes. The top few meters of soil at the Château La Louvière vineyard were qualitatively characterized prior to this study using samples retrieved from five soil pits that ranged in depth from 0 to 2 m below ground surface (Tregoat 2007). Soil samples were sent to a laboratory for analysis, yielding the percent of gravel, sands, silt, clay and organic matter. Pedological expertise was used to interpret and spatially interpolate soil information at this site to yield a pedological map of soil types (Tregoat 2007). A generalized map of the distribution of major soil types within the study zone is given in Fig. 1c, showing the distribution of Calcisol, Colluviosol, Brunisols, and Redoxisol soils. The pedological study suggested that Calcisol underlies about 50% of the study site. Calcisol is a clay-rich soil (> 30%) that has a substantial secondary accumulation of lime. Calcisol is characterized by high water retention capacity and high organic matter. Three variations of Calcisol were identified at the site, including 'Calcisol on shallow carbonate bedrock', 'Calcisol sandy' and 'Calcisol with deeper clay'. The pedological study suggested that approximately 30% of the site is underlain by Colluviosol, which is a deep sandy soil developed on colluvium with low organic matter. Sand content in Colluviosol can be up to 90%. Two types of Colluviosol were identified at the Site, including 'Colluviosol on shallow carbonate bedrock' and 'Colluviosol deeper gravelly sands'. Redoxisol underlies about 8% of the studied area. Redoxisols are sandy soils that are located at low elevation portions of the site and characterized as having roots that are waterlogged in the winter but not in the summer. At this site, the Redoxisol is also interpreted to be underlain by shallow carbonate bedrock (~ 1 m depth). Finally, Brunisols were interpreted to underlie about 12% of the study site. Brunisols are generally composed of sand mixed with more than 50% gravel (diameter > 2 mm) and as such, have a relatively low water-retention capacity. At this study site, the Brunisols are located at higher elevations.

As previously mentioned, it is important to consider the expected root depth zone when designing an experiment intended to study the influence of soils on grapevine properties. At this Château, Tregoat (2007) documented the presence of roots in Calcisols at depths of 1.5 m using soil pits. Dense roots were also described in Colluviosol pits at depths of 1.7 m. Mary et al. (2018, 2020) investigated root behavior in two grapevines in one of the same vineyard blocks of this study using time-lapse geoelectric data collected over 1.5 m depth during an infiltration study. Their interpretation suggested that while the bulk of the active roots were at depths less than 40 cm, there were likely active roots that extended deeper in the section. Their imaging also suggested fairly rapid responses to soil moisture at depths of ~ 1 m in response to the infiltration experiment. These studies suggest that at this site, it is important to use EMI acquisition modes that can interrogate over depths of at least 1 m, and ideally to 1.7 m below ground surface.

The study site for this investigation (Fig. 1c) included a northwest facing parcel of the vineyard, planted with Sauvignon Blanc and Merlot grapevines. The total study parcel measured 360 m × 300 m and included 200 rows of grapevines. The elevation ranged from 35 m above sea level on the southeast part of the site to 20 m on the northwest side. The majority of the lower elevation Sauvignon grapevines in the parcel are ~ 40 years old with some parcels containing grapevines that are 10 years old, while upper grapevine parcels in the study parcel are 15 years old. The lower elevation

portion of the study site tended to have a grass cover crop, whereas the upper elevations had bare soil. The vineyard soils are tilled to a depth of ~20 cm before the summer growing season, and chemical treatments (including copper, sulfur and nitrogen) are applied regularly from end of April through August.

Methods and datasets

The key datasets used for this study were collected in the summers of 2016 and 2017. The main EMI and NDVI datasets used to explore soil–plant property covariability were collected in 2017, as is described below. However, additional supporting datasets were collected at other times to aid in the interpretation of the 2017 EMI data. These supporting datasets included ERT profiles and time domain reflectometry (TDR), both collected June 23, 2016, and soil samples. TDR data were collected to explore shallow soil moisture variability along the ERT transects. Figure 1c shows the location of some of the datasets, including the ERT transects, and soil pit data (P) collected in 2007 as well as hand-augered core soil data (C) collected in 2018. One ERT transect, which was acquired through Sauvignon Blanc grapevines, extended along a 174 m traverse and is referred to as the “Sauvignon transect”. A second ERT transect, which traversed Merlot and Sauvignon Blanc grapevines, extended 230 m; this transect is subsequently referred to as the “Merlot” transect.

The key datasets used to explore spatial covariance of soil and grapevines in this study included EMI and NDVI data, which were collected from June 22–July 8, 2017. This represents a period between mid-flowering and mid-veraison in the Bordeaux region (Bois et al. 2018), when vegetation is still growing and berries are forming. The EMI data were collected to image soil variability and the airborne hyperspectral imaging dataset was collected to image vegetation variability. No thinning of leaves had been performed in the study site prior to this 2017 campaign. During the 2017 campaign, the mean air temperature ranged between 16 and 28 °C and humidity ranged from 68 to 93% (Supplemental Fig. S1). A precipitation event occurred during the 2017 campaign, which brought the cumulative precipitation to approximately the same value as the previous year when the ERT data were collected at the site (Fig. S1). The EMI dataset was collected over the entire study site shown in Fig. 1c, and the hyperspectral dataset was collected over the central portion of the site. Acquisition of the ERT and EMI datasets was carefully designed to sense the entire root zone and to avoid interference from metal or other site infrastructure. The spatial resolution of the EMI and NDVI were chosen to be sufficiently high to enable imaging of natural lateral variability in soil and plant properties, respectively, and to be compatible for joint interpretation. The air temperature and humidity trends were similar during the 2016 and 2017 campaigns (Fig. S1). As no irrigation was performed at this site, and because the cumulative precipitation at the time of the 2016 ERT acquisition campaign was similar to that at the time of the 2017 campaign used to collect EMI datasets, it is assumed that the soil conditions were sufficiently similar to allow use of the depth-resolved 2016 ERT datasets to gain confidence in the averaging depth of the 2017 EMI datasets. A description of the key datasets used in this study is provided below.

Electromagnetic induction data (EMI)

Controlled-source inductive electromagnetic methods consist of injecting a time- or frequency-varying current into a transmitter coil to create a primary electromagnetic field that diffuses to a receiver coil via paths above and below the ground surface. Governed by Maxwell's equations, the created electromagnetic field induces eddy currents in conductors, which in turn creates a secondary magnetic field. A direct estimate of soil ECa is obtained using this ratio of the secondary to the primary magnetic field, the transmitter–receiver (Tx–Rx) distance and the injection current frequency (e.g., McNeill 1980; Telford et al. 1990). A review of electromagnetic methods for shallow subsurface investigations is given by Meju and Everett (2005).

In this study, the CMD Mini-Explorer (GF Instrument, Czech Republic) was used to map the soil ECa. The instrument operates at 30 kHz transmission frequency with three possible receiver coils spacings of 0.3 m, 0.7 m, and 1.2 m, which can be positioned in a horizontal or vertical orientation. Data were acquired using the vertical dipole mode with 1.2 m transmitter–receiver spacing, which had an approximate depth of investigation of 1.8 m (Bonsall et al. 2013), appropriate for studying the root zone at this Château. As with other electromagnetic devices, the Mini-Explorer provides the soil ECa in mS/m and the in-phase ratio in parts per thousand, which is largely determined by the magnetic susceptibility contribution of the soil or by the inductive contribution of the soil and associated metal infrastructure. At this site, there were no metal fences or high wire lines that could cause possible interference with the EMI data. While trellis wires were present, they were not directly connected to the soil and as such, did not contribute to the geophysical signal.

EMI data were collected using a manual mode, with measurements acquired every 3 m along 200 vine rows that were spaced 1 m apart. A Differential Global Positioning System (DGPS) was connected to the Mini-Explorer to simultaneously georeference the measurements. The raw field data were cleaned to delete measurements related to metal objects and access roads at the site. To filter these influences, soil ECa values greater than 100 mS/m and soil ECa values less than 0 mS/m were removed. The remaining dataset was linearly interpolated to obtain an soil ECa distribution map across the studied region (except along access roads) with a pixel size of 2 m by 2 m.

Electrical resistivity tomography (ERT)

ERT surveys typically use a four-electrode measurement approach, in which current is injected between two electrodes and the electrical potential difference is measured between the two others, while varying both the location of electrodes along the profile and the distance between them. Binley and Kemna (2005) provide a review of the ERT method. A Syscal Pro electrical resistivity (Iris Instruments) multichannel (10), multi-electrode (72) device was used to measure the apparent resistivity for this study, employing a Wenner–Schlumberger configuration. The two ERT transects (Fig. 1c) extended 230 m and 174 m, which corresponded to 460 and 348 electrodes, respectively, with 0.5 m spacing between the electrodes.

The distribution of subsurface electrical resistivity was obtained using an inverse modeling approach. The ERT data were inverted using the Boundless Electrical Resistivity Tomography (BERT) code. This method is based on finite element modeling and on a

smoothness-constrained Gauss–Newton inversion. Information about this method is provided in Günther et al. (2006) and in Günther and Rucker (2018).

Soil pit and core-based data

Soil samples were collected for this study using hand drilling equipment in March 2018. During this campaign, 3 cores that extended to a depth up to 2.45 m depth were acquire at sites labeled C1, C2 and C3. Soil textural analysis was performed using a sieve analysis method (Buurman et al. 1996), yielding the percent silt, clay and combined sand and gravel content for each sample. For comparison with the geophysical data, the soil textural data were combined into two categories: one that represented a sum of the silt and clay fractions, and the other that represented the sum of sand and gravel fractions. The results of the textural analysis from samples at the three core sites are shown in Table 1, together with the sum of the textures obtained from Pit (P) soil textural analysis given by Tregoat (2007). Note that Tregoat (2007) also reported the fraction of organic matter as part of the analysis, so the sum of the combined soil texture fractions shown in Table 1 for the P sites are in some cases less than 100%. Also note that the nomenclature of the Tregoat (2007) pit locations were renumbered in this study for simplicity; the correspondences between nomenclature is given in Table S1 (Supplementary Material).

To enable comparison of with EMI data, the depth-averaged percentage (A) of gravel, sand, silt and clay at each sampling location was calculated over the first two meters using:

$$A = \frac{s1 * d1 + s2 * d2 + sn * dn}{dt}, \quad (1)$$

where $s1$, $s2$, and sn correspond to the fraction of soil component at $d1$, $d2$, and dn depth intervals measured during the drilling, and where dt is total depth.

Soil moisture and groundwater level variability was also considered in conjunction with geophysical and coring activities. During March 2018, coring activities visually confirmed that the water table was around 0.7 m below ground surface (BGS) at Soil Pit P2, 1.4 m BGS at Pit P4 and 1.9 m BGS at Pit P5 (Fig. 1c). TDR data were acquired with a Trace system using an 8 cm waveguide along the Merlot and the Sauvignon profiles during the June 2016 campaign. Moisture content, which was estimated using the measured dielectric constant values and Topp's petrophysical relationship (Topp et al. 1980), suggested an average topsoil moisture content of 19.8% along the lower elevation Merlot transect and 16% along the sloped, higher elevation Sauvignon transect. However, as it was difficult to obtain good contact between the TDR waveguides and the soil due to the gravelly nature of the soil, there was high variability in measurements made in close proximity of each other. As such, the TDR measurements are considered to be of low quality and thus were not quantitatively used in this study.

Airborne hyperspectral imaging

Airborne hyperspectral imagery enables land surface imaging using a large number of narrow (≤ 10 nm) and contiguous spectral bands (usually more than 100) (Goetz et al. 1985). The airborne hyperspectral imagery records the spectral response of the ground surface in the visible and near-infrared (VIS–NIR) range of the electromagnetic spectrum. With airborne imaging, individual pixels provide a spectral signature of objects or materials on the ground, such as plants or soils (Ranjan et al. 2016). In addition, by

Table 1 Synthesis of soil texture data obtained from core (C; this study) and pit (P; Tregoat 2007) samples

Core (C) or pit (P) location	Depth interval (cm)	%gravel + sand	%clay + silt
C1	0–7	57.5	42.5
	76–80	46.6	53.4
	89–95	46	54
	120–130	73.8	26.2
	245–250	82.2	17.8
C2	0–6	74.2	25.8
	184–194	69.9	30.1
	210–220	26.3	73.7
C3	37–43	73.1	26.9
	84–90	31	69
	108–114	42.9	57.1
	138–144	35.2	64.8
	154–160	22	78
P1	239–245	10.3	89.7
	0–40	86.3	12.8
	40–100	90.8	8.9
	100–125	38.7	15.7
	125–145	58.6	40.7
P2	145–175	58.2	35.6
	175–210	68.7	30.9
	0–40	72.7	26.6
	40–120	74.8	24.7
	120–170	70.2	29
P3	170–200	71.1	28.2
	0–100	80.5	19
	100–150	89.9	9.7
P4	150–170	68.1	31.5
	0–80	93.2	5.8
	80–120	98.1	1.5
P5	120–> 200	91.4	8.3
	0–60	84.7	13.7
	60–70	21.5	78
	70–150	85.7	14.3

combining specific spectral bands, particular vegetation indices can be obtained that are sensitive to plant vigor, health, and density, including NDVI. A review of NDVI imaging for viticulture is given by Jones and Grant (2018).

In this study, airborne hyperspectral imagery data were acquired using a Basler acA130060gm-NIR camera, which acquires 368 bands in the VIS–NIR range, 450–1300 nm, with a resolution of 3 nm/band. The acquisition took place along 4 axes of the study site parallel to the vineyard rows using an ultralight trike (Pipistrel Sirrus), with a flight altitude of 300 m, and a speed of 80 km/h. The field of view of the camera

was 250 m, with a pixel resolution of ~ 25 (parallel to the vineyard rows) \times 35 cm (perpendicular to the vineyard rows).

NDVI values were estimated using information from hyperspectral information and used to infer grapevine vigor. The index was calculated through a normalization procedure using the wavelengths at the near infrared NIR (860 nm) and red (660 nm) band regions of the electromagnetic spectrum. The formula for estimating NDVI is (Huete 1988):

$$NDVI = \frac{NIR - RED}{NIR + RED} \quad (2)$$

The NDVI is a broadband index, which is generally well defined for multispectral sensors, where each spectral band covers a wide range of the spectrum. In contrast, with hyperspectral imagery, the NIR and red regions include several spectral bands. Two common strategies exist for computing broadband indices, such as NDVI, using hyperspectral data. One strategy consists of averaging the bands within each spectral region, and a second strategy consists of choosing bands that correspond to the central wavelength of each spectral region, such as NIR (860 nm) and red (660 nm). While the NDVI index ranges from -1 and 1 , the range of values that have sensitivity to green vegetation (even for low-vegetation covered areas) is between 0 and 1 , where 1 represents the upper end of green vegetation.

NDVI values estimated using Eq. (2) were further processed by masking pixels related to access roads and interpolating data to a 2 m by 2 m pixel grid to facilitate the comparison with the spatially distributed EMI dataset.

Results and discussion

Soil variability along the ERT transects

Figure 2 shows the inverted electrical conductivity from the Merlot and Sauvignon ERT transects, whose locations are shown in Fig. 1c. The photographs of the soil pits are shown at their corresponding locations along the ERT transects. The locations of the pits and core stations are also shown. The data (Table 1) and pictures show that the soil pits were dominated by sand and gravel down to a depth of ~ 1.5 m below the ground surface. Visual comparison of the ERT data and the soil textures along the Merlot transect (Fig. 2a) indicated that there were generally two distinct ECa responses to two different bulk soil types, or 'soil classes'. The first soil class was characterized by relatively high sand and gravel content (gravel + sand $> 70\%$) and consequently lower soil ECa values (between 5 and 25 mS/m). The second class was characterized by higher clay content with a percentage of clay + silt $> 50\%$ and consequently higher electrical conductivity values (between 25 and 80 mS/m). The second class was mainly observed at the middle of Merlot transect (from $x = 100$ to 150 m at depths $z = 1$ –2 m) (Fig. 2a). Figure 2b shows the Sauvignon ERT transect. This transect was characterized by high electrical conductivity of ~ 50 to 80 mS/m over the top two meters. The soil analysis associated with this transect showed a high percentage of clay and silt with a percentage of clay + silt $> 50\%$ mixed with sand at 1 m depth, and a high percentage of sand between 1 and 2 m depth. Both soil analyses and electrical conductivity values highlighted the presence of an anomaly at $x = 120$ –145 m and with soil electrical conductivity of 5 to 15 mS/m, where there was a high percentage of sand + gravel $> 70\%$ of sand and bedrock carbonate from 0 to 2 m. These visual

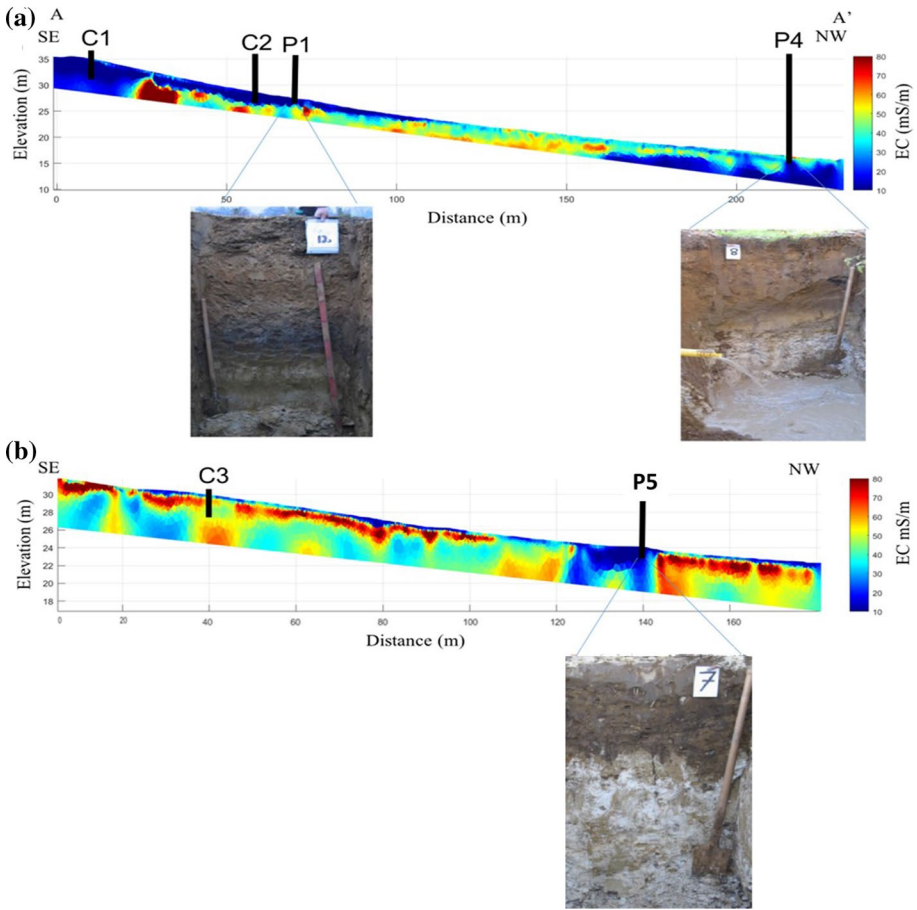


Fig. 2 Locations and examples of soil pits and cores along two ERT transects. Soil texture fractions obtained from analysis of the samples from the soil pits (P) and cores (C) are shown in Table 1. **a** The Merlot ERT transect is characterized by relatively lower electrical conductivity (mS/m) and the four soil pit/core are correspondingly dominated by sand and gravel. **b** The Sauvignon Blanc ERT transect is characterized by relatively higher electrical conductivity (mS/m)

assessments formed the basis of a statistical analysis of the relationship between electrical conductivity and soil texture, which is described below.

Gaining confidence in the value of EMI for providing depth averaged information about soil textures

Figure 3a represents a plan view map of the spatial variability of the soil EC_a (mS/m) obtained from EMI data. The soil EC_a varies between 5 and 55 mS/m and can be divided into three ranges of EC_a values based on visual inspection. The first range includes the lowest soil EC_a values (5 to 20 mS/m), which is located in the Northwest and South of the site. The second range includes intermediate soil EC_a values (20 to 30 mS/m), which is

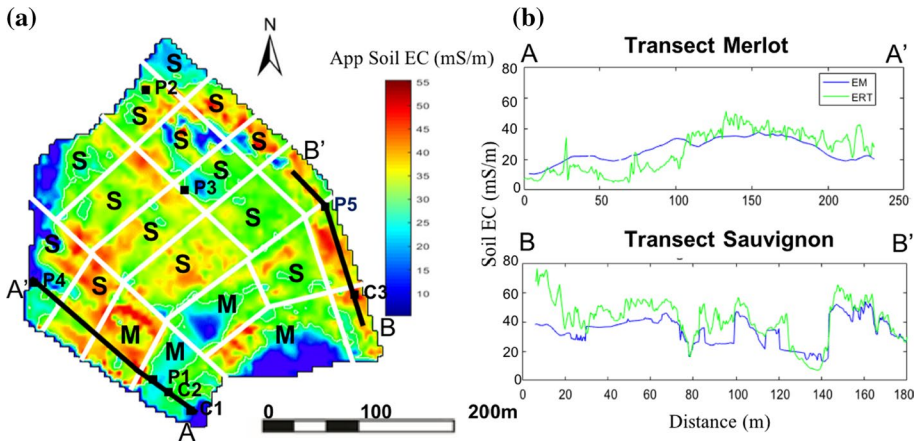


Fig. 3 **a** ECa map (in mS/m) obtained from the EMI data. The two black lines are the positions of the ERT transects: AA' corresponds to the Merlot transect and BB' to the Sauvignon transect. Individual vineyard blocks, planted to Merlot and Sauvignon are indicated by M and S, respectively. The white lines delineate the roads that separate vineyard blocks at the study site. Locations of the Pit (P) and Cores (C) are shown by black dots; **b** comparison of soil electrical conductivity values obtained from ERT and soil ECa obtained from EMI along the two ERT transects

located largely in the center and southeast. The third range comprises the highest soil ECa values (30 to 55 mS/m), which is located largely at East and West of the site.

To take advantage of the spatially extensive ECa information obtained from EMI for understanding soil variability over the expected grapevine root zone, it is important to understand the sensitivity of the EMI method as a function of depth. To investigate this, in this study the ECa estimated from EMI data with electrical conductivity values from ERT that were averaged over the top 2 m below ground surface, a depth that is expected to encompass the majority of the vineyard roots at this study site (Mary et al. 2018). Figure 3b shows the favorable comparison between the inverted and averaged electrical conductivity values obtained from the ERT dataset and the ECa obtained from EMI data at the same locations. Figure 3b transects, labelled A–A' and B–B', show that the trends between the EMI and ERT datasets are very similar, and that the EMI has a smoother trend compared to the averaged ERT electrical conductivity values. An exception is near the southeast end of the Sauvignon transect, where the electrical conductivity estimate from the ERT is higher than the EMI ECa values. The favorable comparison between EMI and averaged ERT electrical conductivity values indicates that the easy-to-acquire EMI dataset should be useful at this site to provide spatially extensive information about soil ECa over the depth range of the grapevine roots.

Estimated Bordeaux soil classes using EMI and soil data

To develop an understanding of the relationship between soil ECa and soil texture at the site, a histogram of soil ECa distribution obtained from the entire EMI data set was analyzed. Figure 4a suggests that the histogram can be divided into three sub-distributions, as indicated by the color coding. Linear regression between the soil ECa values from EMI data and depth averaged soil textural information obtained using Eq. 1 was

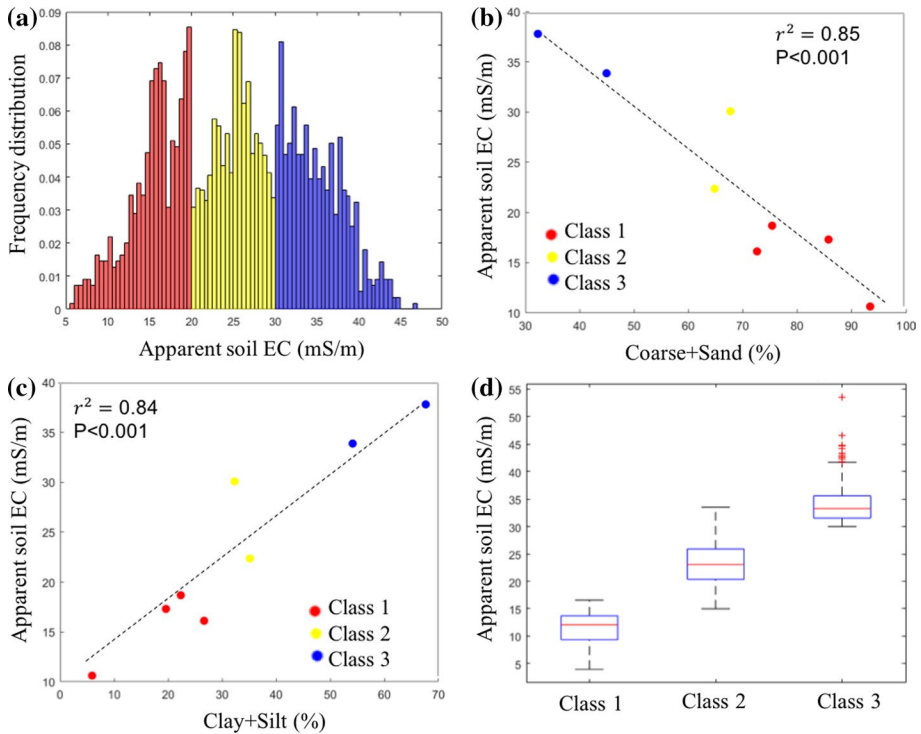


Fig. 4 Soil ECa distributions and relationships between ECa and the sum of depth-averaged soil texture fractions, calculated using Eq. 1, and geophysically-identified Bordeaux Soil Classes (Class1, Class2 and Class3). **a** Frequency distribution of the soil ECa of site, where the colors correspond to those of the symbols shown in Fig. 4b and c. Based on the distribution of ECa as a function of finer and coarser texture fractions, 3 ‘Eca soil classes’ were defined and associated with interpreted Bordeaux soil types. **b** Negative linear correlation between the total depth averaged percentage of clay+silt and soil ECa and **c** positive linear regression between total percentage of gravel+sand and soil ECa; **d** boxplot distribution between ECa from EMI data and geophysically-defined Bordeaux soil Classes

performed on available co-located pit/core samples over the first 2 meters below ground surface (Table 1). For this regression, the EMI ECa value associated with the $2\text{ m} \times 2\text{ m}$ pixel that contained the pits/cores was used. To explore the relationship between electrical signature and ratio of fine to coarse soil texture, the correlations between soil ECa and clay + silt fractions and between soil ECa and gravel/sand fractions were separately analyzed. Figure 4b shows a strong negative correlation between soil ECa values and gravel + sand content ($r^2 = 0.85$, $p < 0.001$) and Fig. 4c shows a strong positive linear correlation between soil ECa values and clay + silt content ($r^2 = 0.84$, $p < 0.001$). These results indicate that the EMI-based ECa information provides information that can be used to distinguish between the finer and coarser fractions of the Bordeaux soils in this vineyard.

To take advantage of the information that the soil ECa provides about soil texture while maintaining relevance to the Bordeaux pedological classifications identified at the Château (Tregat 2007), a correspondence between EC-based soil Classes and the traditional Bordeaux soil types was developed as follows:

- Class 1 is characterized by a high percentage (~70%) of total gravel and sand fraction. The soil ECa values of Class 1 soils range from approximately 5 to 20 mS/m. Class 1 soils are located predominantly to south and north ends of the site. This class corresponds to pedologically interpreted Brunisol, Redoxisol, and Colluviosol underlain by shallow bedrock (a specific kind of Colluviosol as described in Sect. 2). While distinguishing the different pedological classes solely based on their ECa value is not possible, topographic information can potentially provide additional constraints. For example, the low elevation regions of Class 1 soil are composed of Redoxisol, which is typically associated with areas that are wetter than neighboring regions. Brunisol appears in well drained zones (Baize and Girard 2008), which in La Louvière are likely to be the higher elevations.
- Class 2 is characterized by a high percentage (> 60%) of sand fraction, with a soil ECa range of approximately 20 to 30 mS/m. Based on the pedological interpretation, Class 2 soils are composed primarily of Colluviosol, and secondarily of Calcisol.
- Class 3 is composed of Calcisol, which is dominated by the presence of high (> 35%) total clay and silt content. The soil ECa values of Class 3 soils correspond to a range from 30 to 60 mS/m.

Figure 4d shows a boxplot distribution of the three geophysically-defined soil classifications (Class 1, Class 2, and Class 3), which highlights the clear electrical conductivity distinction between the three groups.

The identified soil Class-ECa relationships were used with the EMI based soil ECa data (Fig. 3a) to estimate the spatial distribution of new soil Classes across the study site. Figure 5 shows the resulting distribution of the geophysically-interpreted vineyard soil Classes, plotted using the same pedological colors shown in Fig. 1c to enable comparison

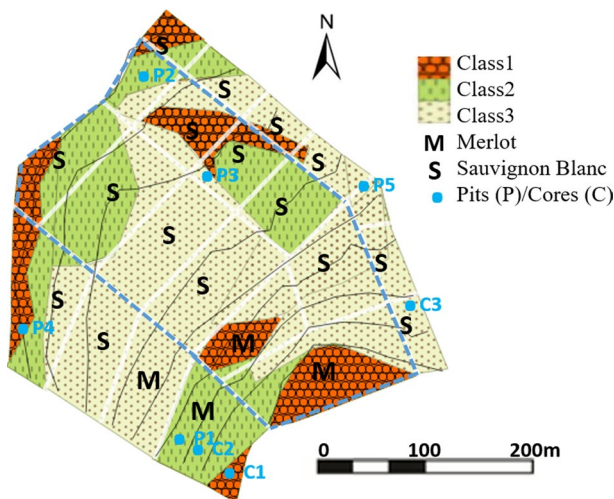


Fig. 5 Distribution of the soil classification within the vineyard area based on EMI data (Fig. 3a) and the relationship between Eca and soil Class (Fig. 4d). The geophysically-identified Bordeaux soil Classes incorporate geophysical information as well as the pedological classes identified at Château La Louvière: Class 1 represents a combination of Brunisol, Redoxisol and Colluviosol on Bedrock; Class 2 is predominantly Colluviosol, Class 3 is predominantly Calcisol. The white lines delineate the roads that separate vineyard blocks at the study site. The blue dashed boundary delineates the region covered by hyperspectral data (see Fig. 6) (Color figure online)

of the pedological and geophysical-identified Bordeaux soil classes. Comparison of the qualitative pedological soil interpretation (Fig. 1b) and the geophysically-driven soil classification (Fig. 5) indicates that there are many similarities and some differences. In general, the geophysical-based soil classification indicates more heterogeneity, presumably reflecting a refined interpretation that is based on high resolution EMI ECa information compared to the pedological interpolation of soil pit data alone.

Estimate grapevine vegetation spatial variability using NDVI

Hyperspectral data were collected during the 2017 growing season over part of the study site identified by the dashed region in Fig. 5. The imaged subregion includes eleven blocks (BL), named BL1 to BL11. The hyperspectral data were interpreted in terms of NDVI using Eq. 2, as shown in Fig. 6. This figure indicates the presence of three categories of NDVI values. Category 1 is characterized by high NDVI values (0.6 to 0.9) or high grapevine vegetation vigor; these grapevines are located mostly in southeastern and northern part of the site within blocks BL2, BL10, and BL11. Category 2 is characterized by intermediate NDVI values (0.4 to 0.6), located primarily in BL3, BL4, BL7, BL8, and BL9. Finally, Category 3 is characterized by low NDVI values (0 to 0.3), which are located mostly in the south of the site in BL1 (Fig. 6). It is interesting to note that the Merlot and Sauvignon Blanc grapevines are not statistically distinguishable based on their NDVI values during the growing season at this study site (data not shown).

Relationship between NDVI and interpreted soil classes

To investigate the extent to which soil texture influenced grapevine vegetation, the NDVI values were statistically compared to the geophysically-estimated Bordeaux soil

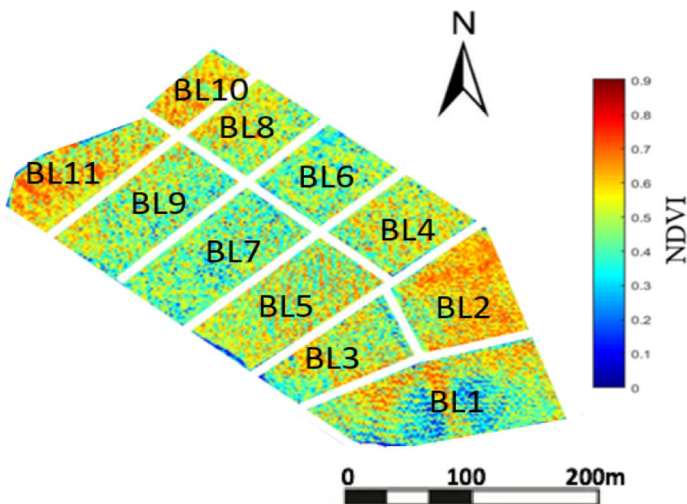


Fig. 6 NDVI map obtained from hyperspectral data collected over the subregion of the study site shown by the blue dashed line in Fig. 5. Blocks (BL) 1–11 correspond to distinct vineyard blocks planted to either Merlot or Sauvignon Blanc as shown in Fig. 5 (Color figure online)

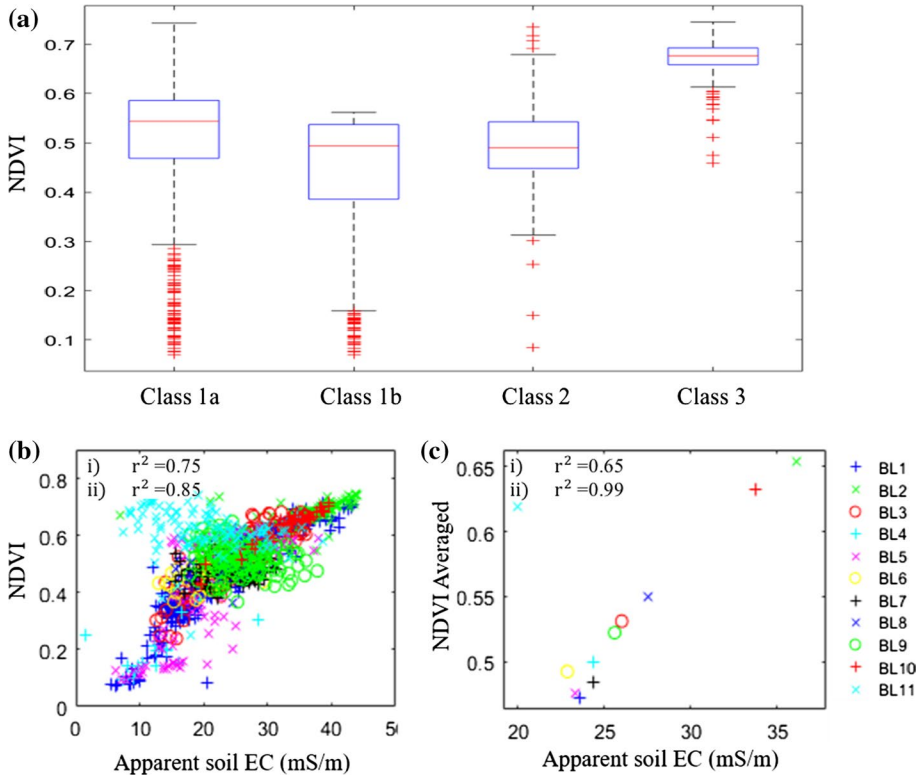


Fig. 7 Statistical analysis of NDVI, soil ECa, and associated geophysically-estimated Bordeaux Soil Classes. **a** Boxplot distribution of NDVI as a function of the three geophysically-estimated soil classes, including minimum, interquartile, median and maximum NDVI values for each soil class. Class 1a and Class 1b include Class 1 data with and without BL11 data, respectively. **b** Cross-plot of soil ECa and NDVI grouped by the different blocks (correlation coefficients with and without BL11 are $r^2=0.75$ and $r^2=0.85$, respectively); **c** cross-plot of block-averaged soil ECa and averaged NDVI (correlation coefficients with and without block 11 are $r^2=0.75$ and $r^2=0.99$, respectively)

classifications. Figure 7a shows a boxplot distribution of NDVI values as a function of geophysically-estimated soil classes. The rationale for exploring the NDVI response of Class 1 that has been split into two subclasses (Class 1a and Class 1b) is described below. Here, the general observations from Fig. 7a are discussed. This graph indicates that Class 1 (1a+ 1b) Bordeaux soils, which had the highest gravel+ sand content (>75%) also had the lowest NDVI (<0.4) values (i.e., the lowest vigor). Class 2 Bordeaux soils, which had intermediate clay (15–20%) and sand (>50) content, also had intermediate NDVI values (0.4 to 0.6). Finally, Class 3 soils, which had the highest clay content, also had the highest NDVI values (>0.6), or the greatest vigor. Higher clay and silt content often leads to higher soil water holding capacity, and higher sand and gravel content soils are usually associated with greater drainage (e.g., Jury and Horton 2004). NDVI did not show a statistical relationship with position along the slope, nor with winegrape varietal (data not shown). These results suggest that at this vineyard location, soil texture influences grapevine vegetation vigor spatial variability during the growing season, with higher NDVI associated with the finest textured soils and lower NDVI associated with the coarsest textured soils. While not

explicitly tested herein, as fine textured soils typically have higher water holding capacity compared to coarser soils, the results also suggest that high grapevine vigor is most associated with the moister soils at this site.

Relationship between NDVI and Soil ECa

In order to explore the spatial variability of the relationship between soil ECa and plant vigor NDVI, their covariability was evaluated as shown in Fig. 7. Linear regression between soil ECa and NDVI pixels was performed separately for each block. The relationship (Fig. 7b) was generally positive and monotonic, with the exception of BL11, which is located at the lowest elevation of the site and near a forested creek. While BL11 was interpreted by the pedologist as a Redoxisol (Tregoa, 2007), as Redoxisols and Brunisols could not be distinguished based on ECa values, they were both categorized as Class 1 textures herein. However, the juxtaposition of BL11 could contribute to root waterlogging, leading to an anomalous ECa-NDVI response compared to other blocks in the study site. While data are not available to test this hypothesis of why BL11 is an outlier, soil Class 1 was separated in two subclasses, Class1a and Class 1b, to explore the influence of the NDVI-ECa relationship with and without B11 data (Fig. 7a). The correlation between soil ECa and NDVI is good when BL11 is included ($r^2=0.75$; $p<0.01$) and excellent when BL11 data are excluded ($r^2=0.85$; $p<0.01$).

Other approaches were also used to explore the relationship between NDVI and Soil ECa. The relationship between the block-averaged soil ECa and block-averaged NDVI was also explored through linear regression (Fig. 7c). In agreement with the previous analysis, the correlation coefficients are different with and without BL11 ($r^2=0.65$; $p<0.01$ and $r^2=0.99$; $p<0.01$, respectively). The analysis suggested that the correlation between NDVI and soil ECa is higher when using NDVI and ECa block average (Fig. 7c). The spatial correlation between the two datasets was calculated using a coefficient of spatial association introduced by Matheron (1965) and a hypothesis testing procedure given by Clifford et al. (1989). Both methods indicate that the spatial correlation between the two datasets is strong and statistically significant (see Table S2, Supplementary Materials).

Conclusions

Determining soil variability as well as the covariability of vineyard soil and grapevine characteristics can be challenging using traditional sampling-based methods due to the high spatial variability of as well as the typically large regions over which such information is needed to inform vineyard management. Working at a Pessac Léognan vineyard south of Bordeaux, a statistical analysis of EMI and soil data was performed to estimate the spatial distribution of Bordeaux soil classes at 2×2 m resolution. Information about the depth sampling of the EMI approach and its sensitivity to soil texture variations was performed through comparing EMI ECa with depth-resolved ERT and soil datasets. After gaining confidence in the value of EMI for imaging over the expected grapevine root depth zone, the EMI data were used with soils data to estimate the distribution of soil Classes at a spatial resolution of 2 m by 2 m. The soil Classes honored the original pedological-based Bordeaux pedological interpretations, and provided more spatially explicit estimates of soil heterogeneity compared to an interpretation based on spatial interpolation of soil pit data.

To test the hypothesis regarding the major influence of soil texture on vegetation vigor variability at the scale of a vineyard block or smaller, the high resolution NDVI data interpreted from airborne hyperspectral data were statistically compared to geophysically-interpreted soil Classes as well as EMI ECa values. Results showed a good correlation between the interpreted soil classes and NDVI, which revealed that the finer texture soil classes had the highest vigor, whereas the coarser textured soil classes (which typically have lower water holding capacity compared to finer soil texture classes) had the lowest vigor during the growing season. A significant linear correlation between EMI ECa values and NDVI was documented using pixel-by-pixel as well as block-by-block comparisons. A significant spatial correlation was also documented using two different approaches. The results suggest that at this site and during the growing season, within-block variations in vegetation vigor were largely influenced by soil texture.

The design of this study explicitly considered several factors that may have hindered previous studies attempting to use EMI and NDVI for characterizing vineyard soil and/or vegetation variability, and provide some ‘best practices’ for vineyard managers and researchers. Many factors were considered in the design, including: campaign period during a phenological stage of the grapevine when vigor would likely be influenced by soil variabilities; soil moisture conditions that allowed ECa discrimination of soil variability; an EMI depth of investigation that was appropriate for imaging over the entire grapevine root zone depth; the characteristic lateral length scales of soil and plant variability relative to EMI and NDVI spatial resolutions; and avoidance from vineyard metal infrastructure that can lead to noise in the geophysical datasets. Other factors, such as the heterogeneity of the soil that was largely distinguishable using EMI and uniform slope aspect of the study site, were also likely factors in the success of this study.

To the author’s knowledge, this is the first demonstration of the use of high-resolution EMI data to estimate Bordeaux soil Classes and the joint use of EMI and NDVI data to quantitatively document a significant spatial co-variability between geophysically-defined Bordeaux soil classes and grapevine vigor. The successful results of this study lay the groundwork for future research directions. For example, the significant correlation between NDVI and soil ECa suggests that vegetation properties during the growing season could be estimated, and possibly predicted, through soil texture information, and that Bordeaux soil texture variability could be potentially estimated using NDVI during the growing season in this region if the conditions that rendered this study successful are met. To test this concept, the relationships developed herein could be applied to NDVI data collected over the entire La Louvière vineyard and used to estimate the spatial distribution of Bordeaux soil classes, if the period and micrometeorological conditions are similar to those of this study. The relationship between EMI and Bordeaux soil classes, and the relationship between soil classes and NDVI could be tested during the same period more broadly across other regions in the Pessac Léognan Appellation known to have the same Bordeaux soil classes. When extending over broader regions, it is likely that topography (elevation and slope aspect) will play a more significant role in vegetation variability than was realized at the vineyard block scale of this study. If extension to other sites and scales is successful, then the methodology developed herein could be performed at other key Appellations having different suites of typical soil classes. The joint use of time-lapse EMI and NDVI datasets could also be explored to investigate how soil–plant relationships and their spatial covariability change in response to weather and management practices.

While vineyards are now starting to collect EMI and NDVI datasets, use of these datasets can be hindered by suboptimal data acquisition parameters and by the inability to quantitatively interpret the data in terms of parameters that are useful for guiding vineyard

management. This study discusses several best practices for data acquisition and interpretation, which if followed are expected to enhance confidence in the use of EMI to provide useful soil information over the grapevine root zone. The study also demonstrates the value of a tractable approach for quantitatively interpreting small-scale (within block) soil-grapevine properties and their covariability. As costs to collect EMI and NDVI decline, and with the increased use of agricultural drones, the approach described here is expected to provide cost-effective, valuable information for precision viticulture strategies and decisions, such as guiding fertilizer applications or replanting decisions and for considering how grapevines will function under future climate conditions.

Supplementary Information The online version of this article (<https://doi.org/10.1007/s11119-021-09788-w>) contains supplementary material, which is available to authorized users.

Acknowledgements The authors thank Château La Louvière for allowing access to the site, as well as for their viticulture insights. Nicola Falco, Yuxin Wu, Susan Hubbard, Baptiste Dafflon and Abdoulaye Balde acknowledge support for this effort from Lawrence Berkeley National Laboratory-Directed Research and Development (LDRD) grant. Myriam Schmutz thanks Pierre Sansjofre for the soil core extractions.

Open Access This article is licensed under a Creative Commons Attribution 4.0 International License, which permits use, sharing, adaptation, distribution and reproduction in any medium or format, as long as you give appropriate credit to the original author(s) and the source, provide a link to the Creative Commons licence, and indicate if changes were made. The images or other third party material in this article are included in the article's Creative Commons licence, unless indicated otherwise in a credit line to the material. If material is not included in the article's Creative Commons licence and your intended use is not permitted by statutory regulation or exceeds the permitted use, you will need to obtain permission directly from the copyright holder. To view a copy of this licence, visit <http://creativecommons.org/licenses/by/4.0/>.

References

- Almaraz, P. (2015). Bordeaux wine quality and climate fluctuations during the last century: Changing temperatures and changing industry. *Climate Research*. <https://doi.org/10.3354/cr01314>.
- Anderson, M. C., Neale, C. M. U., Li, F., Norman, J. M., Kustas, W. P., Jayanthi, H., et al. (2004). Upscaling ground observations of vegetation water content, canopy height, and leaf area index during SMEX02 using aircraft and Landsat imagery. *Remote Sensing of Environment*. <https://doi.org/10.1016/j.rse.2004.03.019>.
- André, F., Saussez, S., Moghadas, D., Van Durmen, R., Delvaux, B., Vereecken, H., et al. (2012). High-resolution imaging of a vineyard in south of france using ground-penetrating radar, electromagnetic induction and electrical resistivity tomography. *Journal of Applied Geophysics*. <https://doi.org/10.1016/j.jappgeo.2011.08.002>.
- Baciocco, A., Davis, R. E., & Jones, G. V. (2014). Climate and Bordeaux wine quality: Identifying the key factors that differentiate vintages based on consensus rankings. *Journal of Wine Research*. <https://doi.org/10.1080/09571264.2014.888649>.
- Baize, D., & Girard, M. (1998). *A sound reference base for soils: The Référentiel Pédologique (The Pedological Repository)*. Paris, France: Institut National de La Recherche Agronomique.
- Baize, D., & Girard, M. (2008). *Référentiel Pédologique (Pedological Reference)*. Paris, France: Association française pour l'étude du sol.
- Binley, A., & Kemna, A. (2005). DC resistivity and induced polarisation methods. In Y. Rubin & S. S. Hubbard (Eds.), *Hydrogeophysics* (Vol. 50, pp. 129–156)., Water Science and Technology Library Dordrecht, Netherlands: Springer.
- Bois, B., Joly, D., Quénot, H., Pieri, P., Gaudillère, J.-P., Guyon, D., Saur, E., van Leeuwen, C. (2018). Temperature-based zoning of the Bordeaux wine region. *Oeno One*. <https://doi.org/10.20870/oenone.2018.52.4.1580>.
- Bonfante, A., Agrillo, A., Albrizio, R., Basile, A., Buonomo, R., De Mascellis, R., et al. (2015). Functional homogeneous zones (fHZs) in viticultural zoning procedure: An Italian case study on Aglianico vine. *Soil*. <https://doi.org/10.5194/soil-1-427-2015>.

- Bonilla, I., De Toda, F. M., & Martínez-Casasnovas, J. A. (2015). Vine vigor, yield and grape quality assessment by airborne remote sensing over three years: Analysis of unexpected relationships in Cv. Tempranillo. *Spanish Journal of Agricultural Research*, 13(2), 1–8.
- Bonsall, J., Fry, R., Gaffney, C., Armit, I., Beck, A., & Gaffney, V. (2013). Assessment of the CMD mini-explorer, a new low-frequency multi-coil electromagnetic device, for archaeological investigations. *Archaeological Prospection*. <https://doi.org/10.1002/arp.1458>.
- Bramley, R. G. V., & Hamilton, R. P. (2007). Terroir and precision viticulture: Are they compatible? *Journal International des Sciences de La Vigne et Du Vin*, 41(1), 1–8.
- Bramley, R. G. V., Ouzman, J., & Boss, P. K. (2011). Variation in vine vigour, grape yield and vineyard soils and topography as indicators of variation in the chemical composition of grapes, wine and wine sensory attributes. *Australian Journal of Grape and Wine Research*. <https://doi.org/10.1111/j.1755-0238.2011.00136.x>.
- Brevik, E. C., & Fenton, T. E. (2015). The effect of changes in bulk density on soil electrical conductivity as measured with the geonics EM-38. *Soil Survey Horizons*. <https://doi.org/10.2136/sh2004.3.0096>.
- Buurman, P., van Lagen, B., & Velthorst, E. J. (1996). *Manual for soil and water analysis*. Leiden, Netherlands: Backhuys Publishers.
- Clifford, P., Richardson, S., & Hemon, D. (1989). Assessing the significance of the correlation between two spatial processes. *Biometrics*, 45, 123–134.
- Coulouma, G., Tisseyre, B., & Lagacherie, P. (2010). Is a systematic two-dimensional emi soil survey always relevant for vineyard production management? A test on two pedologically contrasting mediterranean vineyards. In R. Viscarra Rossel, A. McBratney, & B. Minasny (Eds.), *Proximal soil sensing. Progress in soil science*. Dordrecht, Netherlands: Springer. https://doi.org/10.1007/978-90-481-8859-8_24.
- Cunha, M., Marçal, A. R. S., & Silva, L. (2010). Very early prediction of wine yield based on satellite data from vegetation. *International Journal of Remote Sensing*, 31, 3125–3142.
- Dafflon, B., Oktem, R., Peterson, J., Ulrich, C., Tran, A. P., Romanovsky, V., et al. (2017). Coincident aboveground and belowground autonomous monitoring to quantify covariability in permafrost, soil, and vegetation properties in arctic Tundra. *Journal of Geophysical Research: Biogeosciences*, 122(6), 1321–1342.
- Das, B. S., Ray, S., Sarathjith, M. C., Santra, P., Sahoo, R. N., & Srivastava, R. (2015). Hyperspectral remote sensing: Opportunities, status and challenges for rapid soil assessment in india hyperspectral remote sensing: Opportunities, status and challenges for rapid soil assessment in India. *Current Science*, 108(5), 860–868.
- Falco, N., Wainwright, H., Dafflon, B., Léger, E., Peterson, J., Steltzer, H., et al. (2019). Investigating microtopographic and soil controls on a mountainous meadow plant community using high-resolution remote sensing and surface geophysical data. *Journal of Geophysical Research: Biogeosciences*. <https://doi.org/10.1029/2018JG004394>.
- Goetz, A. F. H., Vane, G., Solomon, J. E., & Rock, B. N. (1985). Imaging spectrometry for earth remote sensing. *Science*. <https://doi.org/10.1126/science.228.4704.1147>.
- Goulet, E., & Barbeau, G. (2006). Contribution of soil electrical resistivity measurements to the studies on soil/grapevine water relations. *Journal International des Sciences de la Vigne et du Vin*. <https://doi.org/10.20870/oeno-one.2006.40.2.875>.
- Grote, K., Alger, C., Bridget, K., Hubbard, S., & Rubin, Y. (2010). Characterization of soil water content variability and soil texture using GPR groundwave techniques. *Journal of Environmental and Engineering Geophysics*. <https://doi.org/10.2113/JEEG15.3.93>.
- Grote, K., Hubbard, S., & Rubin, Y. (2003). Field-scale estimation of volumetric water content using ground-penetrating radar ground wave techniques. *Water Resources Research*. <https://doi.org/10.1029/2003WR002045>.
- Günther, T., & Rücker, C. (2018). Boundless electrical resistivity tomography. <http://resistivity.net/berl/>.
- Günther, T., Rücker, C., & Spitzer, K. (2006). Three-dimensional modelling and inversion of dc resistivity data incorporating topography-II Inversion. *Geophysical Journal International*. <https://doi.org/10.1111/j.1365-246X.2006.03011.x>.
- Hall, A., Lamb, D. W., Holzapfel, B., & Louis, J. (2002). Optical remote sensing applications in viticulture—A review. *Australian Journal of Grape and Wine Research*. <https://doi.org/10.1111/j.1755-0238.2002.tb00209.x>.
- Hedley, C.B., Yule, I.Y., Eastwood, C.R., Shepherd, T.G. & Arnold, G. (2004). Rapid identification of soil textural and management zones using electromagnetic induction sensing of soils. *Australian Journal of Soil Research*, 42, 389–400.
- Heil, K., & Schmidhalter, U. (2017). The application of EM38: Determination of soil parameters, selection of soil sampling points and use in agriculture and archaeology. *Sensors*. <https://doi.org/10.3390/s17112540>.

- Hubbard, S., Grote, K., & Rubin, Y. (2002). Mapping the volumetric soil water content of a California vineyard using high-frequency GPR ground wave data. *The Leading Edge*. <https://doi.org/10.1190/1.1490641>.
- Hubbard, S., Lunt, I., Grote, K., & Rubin, Y. (2006). Vineyard soil water content: Mapping small scale variability using ground penetrating radar. In R. W. Macqueen & L. D. Meinert (Eds.), *Fine wine and terroir—The geoscience perspective*. St. Johns, Newfoundland: Geoscience Canada Reprint Series Number 9, Geological Association of Canada.
- Huete, A. R. (1988). A soil-adjusted vegetation index (SAVI). *Remote Sensing of Environment*, 25(3), 295–309.
- Imre, S. P., Mauk, J. L., Bell, S., & Dougherty, A. (2013). Mapping grapevine vigour, topographic changes and lateral variation in soils. *Journal of Wine Research*. <https://doi.org/10.1080/09571264.2012.712811>.
- Johnson, L. F., Roczen, D. E., Youkhana, S. K., Nemani, R. R., & Bosch, D. F. (2003). Mapping vineyard leaf area with multi-spectral satellite imagery. *Computer and Electronics in Agriculture*, 38, 33–44.
- Jones, H. G., & Grant, O. M. (2018). Remote sensing and other imaging technologies to monitor grapevine performance. In H. Geros, M. Manuela Chavres, H. Madrano Gil, & S. Delrot (Eds.), *Grapevine in a changing environment* (pp. 179–196). West Sussex, UK: H. Wiley and Sons Ltd. <https://doi.org/10.1002/9781118735985.ch8>.
- Jury, W. A., & Horton, R. (2004). *Soil physics*. New York, USA: Wiley.
- Lamb, D., Mitchell, A., & Hyde, G. (2005). Vineyard trellising with steel posts distorts data from EM soil surveys. *Australian Journal of Grape and Wine Research*. <https://doi.org/10.1111/j.1755-0238.2005.tb00276.x>.
- Lanyon, D. M., Cass, A., & Hansen, D. (2004). The effect of soil properties on vine performance CSIRO *Land and Water Technical Report No. 34/04*.
- Lunt, I. A., Hubbard, S., & Rubin, Y. (2005). Soil moisture content estimation using ground-penetrating radar reflection data. *Journal of Hydrology*, 307, 254–269.
- Mary, B., Peruzzo, L., Boaga, J., Cenni, N., Schmutz, M., Wu, Y., et al. (2020). Time-lapse monitoring of root water uptake using electrical resistivity tomography and mise-à-la-masse: A vineyard infiltration experiment. *Soil*, 6, 95–114. <https://doi.org/10.5194/soil-6-95-2020>.
- Mary, B., Peruzzo, L., Boaga, J., Schmutz, M., Wu, Y., Hubbard, S. S., et al. (2018). Small-scale characterization of vine plant root water uptake via 3-D electrical resistivity tomography and mise-à-la-masse method. *Hydrology and Earth System Sciences*. <https://doi.org/10.5194/hess-22-5427-2018>.
- Matheron, G. (1965). *Les variables régionalisées et leur estimation: une application de la théorie des fonctions aléatoires aux sciences de la nature (Regionalized variables and their estimation: An application of the theory of random functions to the natural sciences)*. Paris, France: Masson.
- McNeill, J. D. (1980). *Electrical conductivity of soils and rocks*. Mississauga, Ontario, Canada: Geonics Limited.
- Meju, M. A., & Everett, M. E. (2005). Near-surface controlled-source electromagnetic induction: Background and recent advances. In Y. Rubin & S. S. Hubbard (Eds.), *Hydrogeophysics* (Vol. 50, pp. 157–183), Water Science and Technology Library Dordrecht, Netherlands: Springer.
- Parker, A. A., de Cortazar-Atauri, I. G., van Leeuwen, C., & Chuin, I. (2011). I. General phenological model to characterise the timing of flowering and veraison of *Vitis vinifera* L. *Journal of Grape and Wine Research*. <https://doi.org/10.1111/j.1755-0238.2011.00140.x>.
- Proffitt, T., & Campbell-Clause, J. (2012). *Managing grapevine nutrition and vineyard soil health*. http://sustainableagriculture.pertregionnrm.com/sites/default/files/Managin_Grapevine%20_Nutrition_Soil_Health.pdf.
- Ranjan, A. K., Vallisree, S., & Singh, R. K. (2016). Role of geographic information system and remote sensing in monitoring and management of urban and watershed environment: Overview. *Journal of Remote Sensing & GIS*, 7(2), 60–73.
- Rodriguez Perez, J.R., Plant, R.E., Lambert, J., & Smart, R.R. (2011). Using apparent soil electrical conductivity (ECA) to characterize vineyard soils of high clay content. *Precision Agriculture*. <https://doi.org/10.1007/s1119-011-9220-y>
- Rudolph, S., Van der Kruk, J., von Hebel, C., Ali, M., Herbst, M., Montzka, C., et al. (2015). Linking satellite derived LAI patterns with subsoil heterogeneity using large-scale ground-based electromagnetic induction measurements. *Geoderma*, 241–242, 262–271.
- Smart, D. R., Schwass, E., Lasko, A., & Morano, L. (2006). Grapevine rooting patterns: A comprehensive analysis and a review. *American Journal of Enology and Viticulture*, 57, 89–104.
- Stednick, J. D., Green, T. R., Buchleiter, G. W., McCutcheon, M. C., & Farahani, H. J. (2006). Effect of soil water on apparent soil electrical conductivity and texture relationships in a dryland field. *Biosystems Engineering*, 94(1), 19–32.

- Sun, L., Gao, F., Anderson, M. C., Kustas, W. P., Alsina, M., Sanchez, L., et al. (2017). Daily mapping of 30 m LAI and NDVI for grape yield prediction in California vineyards. *Remote Sensing*, 9(4), 317.
- Telford, W. M., Geldart, L. P., & Sheriff, R. E. (1990). *Applied geophysics*. Cambridge: Cambridge University Press.
- Topp, G. C., Davis, J. L., & Annan, A. P. (1980). Electromagnetic determination of soil water content: Measurement in coaxial transmission lines. *Water Resources Research*, 16(3), 574–582.
- Tregoat, O. (2007). Cartographie des sols du vignoble de Château la Louvière (Mapping of the soils of the Château la Louvière vineyard). Unpublished report.
- van Leeuwen, C., & Chery, P. (2001). Quelle Methode Pour Caracteriser et Etudier Le Terroir Viticole : Analyse de Sol, Cartographie Pedologique Ou Etude Ecophysiologique? (Which Method To Characterize And Study The Viticultural Terroir: Soil Analysis, Pedological Mapping Or Ecophysiological Study?). *Journal International des Sciences de La Vigne et du Vin*, 35, 13–20.
- Van Leeuwen, C., Friant, P., Chone, X., Tregoat, O., Koundouras, S., & Dubourdieu, D. (2004). Influence of climate, soil and cultivar on terroir. *American Journal of Enology and Viticulture*, 55, 207–217.
- van Leeuwen, C., & Seguin, C. (2007). The concept of terroir in viticulture. *Journal of Wine Research*. <https://doi.org/10.1080/09571260600633135>.
- von Hebel, C., Matveeva, M., Verweij, E., Rademske, P., Kaufmann, M. S., Brogi, C., et al. (2018). Understanding soil and plant interaction by combining ground-based quantitative electromagnetic induction and airborne hyperspectral data. *Geophysical Research Letters*. <https://doi.org/10.1029/2018GL078658>.
- White, R. E. (2015). *Understanding vineyard soils*. New York: Oxford University Press.
- Wilson, J. E. (1998). *Terroir: The role of geology, climate and culture in the making of French wines*. Berkeley, California: University of California Press.
- Wolpert, J. A., & Vilas, E. P. (1992). Estimating vineyard yields: Introduction to a simple, two-step method. *American Journal of Enology and Viticulture*, 43, 384–388.

Publisher's Note Springer Nature remains neutral with regard to jurisdictional claims in published maps and institutional affiliations.